RNase R is associated in a functional complex with the RhpA DEAD-box RNA helicase in *Helicobacter pylori*

Alejandro Tejada-Arranz [1,2], Rute G. Matos[3], Yves Quentin[4], Maxime Bouilloux-Lafont[1], Eloïse Galtier[1], Valérie Briolat[5], Etienne Kornobis[5,6], Thibaut Douché[7], Mariette Matondo[7], Cecilia M. Arraiano[3], Bertrand Raynal[8] and Hilde De Reuse [1,*]

[1]Unité Pathogenèse de Helicobacter, CNRS UMR 2001, Département de Microbiologie, Institut Pasteur, 75724 Paris Cedex 15, France, [2]Université de Paris, Sorbonne Paris Cité, 75006 Paris, France, [3]Instituto de Tecnologia Química e Biológica António Xavier, Universidade Nova de Lisboa, 2780-157 Oeiras, Portugal, [4]Laboratoire de Microbiologie et de Génétique Moléculaires (LMGM), Centre de Biologie Intégrative (CBI), Université de Toulouse, UMR CNRS 5100, 31062 TOULOUSE Cedex 9, France, [5]Biomics, C2RT, Institut Pasteur, 75724 Paris Cedex 15, France, [6]Hub Bioinformatique et Biostatistique, Département de Biologie Computationelle, USR CNRS 3756, Institut Pasteur, 75724 Paris Cedex 15, France, [7]Plateforme Protéomique, Unité de Spectrométrie de Masse pour la Biologie, C2RT, USR CNRS 2000, Institut Pasteur, 75724 Paris Cedex 15, France and [8]Plateforme de biophysique moléculaire, UMR CNRS 3528, Département de Biologie structurale et chimie, Institut Pasteur, 75724 Paris Cedex 15, France

ABSTRACT

Ribonucleases are central players in post-transcriptional regulation, a major level of gene expression regulation in all cells. Here, we characterized the 3′-5′ exoribonuclease RNase R from the bacterial pathogen *Helicobacter pylori*. The 'prototypical' *Escherichia coli* RNase R displays both exoribonuclease and helicase activities, but whether this latter RNA unwinding function is a general feature of bacterial RNase R had not been addressed. We observed that *H. pylori Hp*RNase R protein does not carry the domains responsible for helicase activity and accordingly the purified protein is unable to degrade *in vitro* RNA molecules with secondary structures. The lack of RNase R helicase domains is widespread among the *Campylobacterota*, which include *Helicobacter* and *Campylobacter* genera, and this loss occurred gradually during their evolution. An *in vivo* interaction between *Hp*RNase R and RhpA, the sole DEAD-box RNA helicase of *H. pylori* was discovered. Purified RhpA facilitates the degradation of double stranded RNA by *Hp*RNase R, showing that this complex is functional. *Hp*RNase R has a minor role in 5S rRNA maturation and few targets in *H. pylori*, all included in the RhpA regulon. We concluded that during evolution, *Hp*RNase R has co-opted the RhpA helicase to compensate for its lack of helicase activity.

INTRODUCTION

Ribonucleases (RNases) are important enzymes for many biological processes; their functions are often essential for normal growth, as illustrated by RNase E in *Escherichia coli* or RNase J in *Helicobacter pylori* (1). Many RNases act in concert with other enzymes, like the protein complex that is known as the bacterial RNA degradosome. These latter complexes are composed of at least one RNase and one DEAD-box RNA helicase, although other components have been found in different organisms (1).

We have previously characterized the minimal RNA degradosome of the gastric pathogen *H. pylori* composed of the essential ribonuclease RNase J and the DEAD-box helicase RhpA (2). This bacterium is a mesophilic pathogen that belongs to the phylum of the *Campylobacterota* [formerly termed *Epsilonproteobacteria* (3,4)]. *H. pylori* colonizes the stomach of half of the human population worldwide and this infection leads to the development of gastric pathologies such as peptic ulcers or, in the worst cases, gastric adenocarcinoma, the latter causing up to 800 000 deaths every year (5). *H. pylori* possesses a small genome of 1.6 Mb, that encodes very few transcriptional regulators (6). Therefore, it has been proposed that post-transcriptional regulation plays an important role in the regulation of gene expression of this microorganism, which was confirmed by different studies including those of our laboratory (7,8,9). The minimal RNA degradosome of *H. pylori* is composed of the essential endo- and 5′-3′ exoribonuclease RNase J and the sole DEAD-box RNA helicase encoded in its genome, called RhpA (2,10). These two proteins interact and stimulate each other's activity *in vitro* (2). In addition, they cop-

urify with ribosomes (2), localize at the inner membrane of *H. pylori* and form foci that have been hypothesized to be active degradation hubs (11).

Very little is known on the other ribonucleases of *H. pylori*. Only two 3′-5′ exoribonucleases, the predicted RNase R (*Hp*RNase R) and the polynucleotide phosphorylase (PNPase), are present in the *H. pylori* genome which suggests limited functional redundancy in this organism. In contrast, *Escherichia coli* possesses, in addition to PNPase, two exoribonucleases from the RNB family, namely RNase R and RNase II. While in *E. coli* these two latter proteins are well characterized, there is some confusion in their assignment in other organisms as their sequences present significant similarities.

In *E. coli*, RNase R (12,13) (*Ec*RNase R) plays an important role in the maturation of rRNAs (14), that can act in concert with Hfq (15); in the functionality of *tm*RNA, the major actor of *trans*-translation (16,17); as well as a minor role in mRNA decay (12,18). However, this enzyme is generally thought to be more important for ribosome quality control, as it degrades nonfunctional rRNAs and tRNAs (13,17,19). In *Streptococcus pneumoniae*, RNase R regulates the amount of translating ribosomes (20,21). In *E. coli*, the two other 3′-5′ exoribonucleases, PNPase and RNase II, play a more important role in mRNA decay (22) as well as in tRNA processing (23) and rRNA degradation under specific conditions (24).

In general, RNases are not efficient in degrading structured RNAs by themselves. However, *Ec*RNase R has been found to possess a helicase activity in addition to its 3′-5′ exoribonuclease function (25). Accordingly, *Ec*RNase R can degrade highly structured RNAs such as tRNAs (26), 23S and 16S rRNAs (27). Both activities of *Ec*RNase R are important for its function in cells, as mutations in the Walker motifs (required for helicase activity) or in the RNase active site render it less active (18,28). The helicase activity of *Ec*RNase R was found to be independent of the RNase active site but this activity contributes to efficient ribonuclease activity (29), allowing it to degrade a wider range of substrates (30). Whether the helicase activity is a general feature of bacterial RNase R has not been addressed yet.

The functional domains of *Ec*RNase R are well defined. This protein is composed of a helix-turn helix (HTH) domain at the N-terminal region, followed by two cold-shock domains (CSD1 and CSD2), an RNB domain, a S1 domain and a C-terminal K/R-rich basic domain (Figure 1A). The RNase activity resides in the RNB domain (31), whereas its helicase activity depends on two Walker motifs A and B (ATP-binding sites) that are present in the K/R-rich and CSD2 domains, respectively (29). In addition, the region responsible for the unwinding of the RNA strands (but not for RNA binding or hydrolysis) was mapped to the RNB domain and was termed the tri-helix wedge (32). The S1 domain has also been shown to be important for ATP and dsRNA binding (30) and dsRNA degradation (33,34).

*Ec*RNase R is upregulated upon cold-shock (16,35) and under other conditions such as stationary phase (36). This protein can also be stabilized by its interaction with ribosomal proteins (37,38). In stationary phase, *Ec*RNase R is a minor component of the RNA degradosome (39).

RNase R is also associated with the degradosome of the psychrotrophic bacterium *Pseudomonas syringae* (40).

In *H. pylori*, the *rnr* gene predicted to encode *Hp*RNase R was identified and the corresponding protein shown to display 3′-5′ exoribonuclease activity (41). In that study, six virulence-related genes were found to be downregulated by this RNase, including motility and chemotaxis-related genes and apoptosis-inducing genes. In addition, it was reported that an *H. pylori* Δ*rnr* mutant is more motile and more effective in inducing apoptosis in gastric cells (41). This study also reports that the *rnr* transcript is slightly increased upon cold-shock and repressed upon acid stress. In contrast, we previously found that the *E. coli Ec*RNase R mutant is impaired in motility (42).

We recently addressed the activity of RNase R from *Campylobacter jejuni*, an organism phylogenomically close to *H. pylori* (26). We showed that *Cj*RNase R is active on several substrates, including a residual activity on a perfectly complementary dsRNA substrate, although the helicase activity of *Cj*RNase R was not directly addressed. In addition, *Cj*RNase R was found to be important for *C. jejuni* adhesion and invasion of eukaryotic cells (26).

Here, we defined the functional domains of the *H. pylori* RNase R protein and explored its function by defining its interacting partners and assessing its helicase activity. We found that *Hp*RNase R, like many of its homologues from the *Campylobacterota* phylum, does not possess the helicase signature motifs and demonstrated that it is devoid of helicase activity. Most interestingly, *Hp*RNase R physically interacts with RhpA, the sole DEAD-box RNA helicase of *H. pylori.* Using RNA-Seq, we found an overlap between the few *Hp*RNase R targets and those of RhpA. We concluded that during evolution, *Hp*RNase R has co-opted the RhpA helicase to compensate for its lack of helicase activity.

MATERIALS AND METHODS

Strains and growth conditions

The *H. pylori* strains used in this study (Supplementary Table S1) are derived from strain B128 (43,44). *H. pylori* was grown on Blood Agar Base 2 (Oxoid) plates supplemented with 10% defibrinated horse blood with an antibiotic-antifungal cocktail (2.5 μg.ml⁻¹ amphotericin B, 0.31 μg.ml⁻¹ polymyxin B, 6.25 μg.ml⁻¹ trimethoprim and 12.5 μg.ml⁻¹ vancomycin). Selection of *H. pylori* mutants was performed using 10 μg.ml⁻¹ apramycin or 20 μg.ml⁻¹ kanamycin. For liquid culture, Brucella broth supplemented with 10% fetal bovine serum (FBS, Eurobio) and antibiotic-antifungal cocktail was used. *H. pylori* was grown at 37°C under microaerophilic conditions (6% O_2, 10% CO_2, 84% N_2) generated with an Anoxomat (MART Microbiology) atmosphere generator.

Escherichia coli strains (listed in Supplementary Table S1) were cultured in LB with appropriate selection antibiotics (40 μg/ml kanamycin, 25 μg/ml chloramphenicol and/or 100 μg/ml ampicillin) at 37°C.

Growth curves were performed in 1 ml of Brucella broth supplemented with 10% FBS and antibiotic cocktail, in 24-well plates with a Spark microplate reader (TECAN) at 37°C, 150 rpm and under an atmosphere containing 10%
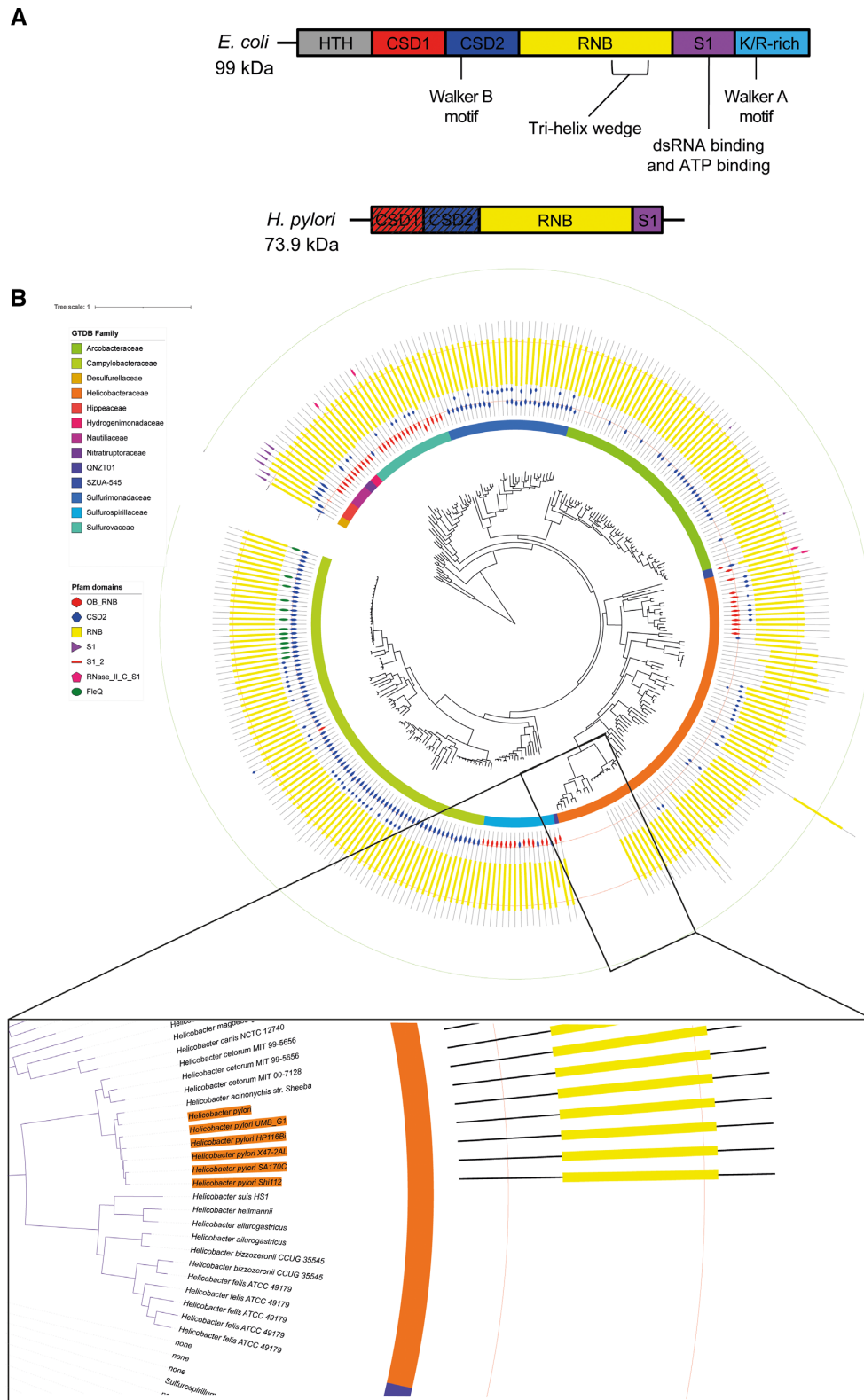
Figure 1. (**A**) Schematic representation of the functional domain organization of *E. coli* RNase R (*Ec*RNaseR) and *H. pylori* RNase R (*Hp*RNase R). The CSD1 and CSD2 domains of *Hp*RNase are hatched to illustrate the poor conservation of these regions compared with *Ec*RNaseR. (**B**) Phylogenic tree illustrating the evolution and conservation of the characteristic domains of RNase R. (For more details, see supplementary Figure S2). The tree species has been pruned to preserve only strains with full-sized proteins, while retaining strains of the genus *Helicobacter* E from GTDB that do not code for RNase R. The names of strains of the *H. pylori* species are highlighted in orange. The GTDB Taxonomy Family Rank has been used as a color code. The location of the pfam profiles predicted with *hmmscan* is reported on the sequences represented by black lines. Note that the first cold-shock domain (CSD1) can also be annotated OB_RNB or CSD2 in Pfam profiles. Details of the data for the *Helicobacteraceae* family are magnified on the bottom part of the figure. The figure was obtained with the *iTOL* v5 software (https://itol.embl.de).

CO_2 and measuring the optical density at 600 nm every hour.

Molecular techniques

Molecular biology experiments were performed according to standard procedures (45) and the supplier (ThermoFisher Scientific) recommendations. Plasmids pET28-RhpA and pET28-*Hp*RNase R were constructed using standard procedures and the primers listed in Supplementary Table S2, adding a TEV (Tobacco Etch Virus) clivage site between the His-tag and the protein sequences. Point mutation D231N was introduced into the pET28-*Hp*RNase R plasmid by using overlapping PCR with the primers listed in Supplementary Table S2 and was verified by sequencing. Plasmid preparations were carried out with the QIAprep Spin Miniprep Kit (QIAGEN) and *H. pylori* genomic DNA extractions were done with QIAamp DNA Mini Kit (QIAGEN). PCR were performed with either DreamTaq DNA polymerase (Thermofisher) or Q5 High fidelity DNA polymerase (NEB) when the product required high fidelity amplification.

Construction of *H. pylori* mutants

Chromosomal deletions of the complete genes encoding RNase R (HPB8_232) and RhpA (HPB8_1316) was performed in *H. pylori* strain B128. Fragments of 500 bp up and downstream of the target gene were amplified by PCR (primers are listed in Supplementary Table S2) and fused with a non-polar apramycin resistance cassette by using the isothermal assembly technique (46) followed by PCR amplification using the primers from the extremities. For HA-tagging at the C-terminus of RNase R, the last 500 bp of *rnr* were amplified with an HA-tag at the end, and were fused with a non-polar kanamycin resistance cassette and a PCR fragment of the 500 bp downstream from *rnr* by isothermal assembly followed by PCR with the flanking primers. All *H. pylori* mutants were obtained by natural transformation [as described in (47)] with the PCR fragments obtained above. Selection of chromosomal allelic exchange resulting in cassette insertion was performed with the appropriate antibiotic. Deletion of the genes of interest and/or insertion of cassettes was verified by PCR and sequencing of the region of interest.

Structural alignment

Multiple alignment of RNB proteins was performed with T-COFFEE Version_11.00 (48). Secondary structure and Pfam domain organization were obtained from Uniprot. Supplementary Figure S1 was created with the *Jalview* software version 2.11.1.3 (49).

Phylogenomics analyses

The sequence dataset was constructed based on the entries annotated as reference genomes of the *Campylobacterota* from the taxonomic classification of the GTDB (release 05-RS95, https://gtdb.ecogenomic.org/) (50) and genomes were extracted from NCBI. The dataset of 322 reference genomes, includes 78 complete genomes, 5 annotated as chromosomes, 86 are composed of scaffolds and 153 of contigs. Taking into account all reference genomes allows a more complete description of the *Campylobacterota* diversity. Genomes were annotated with the Prokka software 1.13.3 (51) and a functional protein annotation was performed with *hmmscan* [HMMER 3.1b2 package (52)] using two sources of HMM: Pfam 32 (https://pfam.xfam.org/) and Hamap 2020_01 (https://hamap.expasy.org/).

The phylogenetic tree of the *Campylobacterota* strains was based on the concatenation of alignments obtained for a set of 120 conserved families of protein sequences, using the cleaned alignment available on the GTDB database. The tree was inferred with *fasttree* version 2.1.10 SSE3 (53), under the LG+GAMMA model and local branch support values were determined using the Shimodaira–Hasegawa test. The tree was rooted from the GTDB taxonomy and drawn with *iTOL* v5 (54).

RNase R protein candidates were identified by the presence of a domain PF00773 (RNB https://pfam.xfam.org/family/PF00773) in the *hmmscan* annotations (297 proteins). They were assigned as RNase R orthologs by *blastp* (BLAST 2.7.1+ package) against the RNB domain sequences of RNases R and II from *E. coli* followed by comparison of the *blastp* scores. All proteins showed better score with *Ec*RNase R than with *Ec*RNase II, except one (AaklB78.g_00001), where the alignment is shorter with RNase R than with RNase II but with a higher sequence conservation with RNase R. Genomes lacking a member of this protein family were further interrogated by *tblastn* (BLAST 2.7.1+ package) using RNase R from *E. coli* as a query.

The analysis of the conservation protein domains was performed using the Pfam annotation with a permissive threshold (e-value <1) to retain annotations from degenerated domains. Results were presented on the tree of species.

Proteins homologous to the DEAD-box RNA helicase were identified using profile PF0027 with the *hmmscan*, followed by filtering and classification using the sequences from the DEAD-box RNA helicases from *E. coli* (DbpA, DeaD, RhlB, RhlE and SrmB) with *phmmer* of the HMMER 3.1b2 package. Sequences of proteins classified as DEAD were aligned with *mafft* v7.453 [–maxiterate 1000 –reorder –localpair (55)], the alignment was trimmed with *trimAl* v1.4.rev22 [-automated1 (56)] and a tree was constructed with *fasttree* version 2.1.10 SSE3 (LG+GAMMA model). On this tree, we identified two groups of paralogous sequences in the *Sulfurovaceae*, one group of which has been named CsdAS to distinguish it from the CsdA family of proteins. Hamap profiles MF_01491 (for bacterial RNase J) and MF_01595 (for PNPase) were used to identify proteins from the RNase J and PNPase families, respectively. The e-value thresholds were set to exclude false positives. As above, *tblastn* was used to search for homologues in the genomes without hits with these profiles.

The distribution of the presence of homologous genes to those encoding the CsdA, RNase R, RNase J and PNPase protein families was grouped at the level of the GTDB taxonomy family. For *Helicobacteraceae*, we have lowered to the genus level.

Protein expression and purification

RNase R from *E. coli* was expressed and purified as described in (57). Plasmids expressing *Hp*RNase R WT, D231N and pET28-RhpA were transformed into *E. coli* BL21 (DE3) Δ*rnb*Δ*rnr* cells for recombinant protein expression. Cells were grown in LB medium supplemented with 50 μg/mL kanamycin at 30°C to an OD_{600 nm} of 0.5. Then, protein expression was induced by the addition of 0.5 mM IPTG and bacteria were grown for an extra 16 h. Cells were pelleted by centrifugation and stored at -80°C. To co-purify *Hp*RNase R with RhpA, cultures overexpressing each protein separately were pelleted together. The pellets were resuspended in 10 mL of buffer A (25 mM Tris–HCl pH 7.5, 300 mM NaCl, 10 mM imidazole) and lysed using the FastPrep-24 (MP Biomedical) at 6.5 m/s for 60 s in the presence of 0.5 mM PMSF. The crude extract was clarified by a 30 min centrifugation at 10 000 g and treated with Benzonase (Sigma) to degrade the nucleic acids. The cleared lysate was subjected to a histidine affinity chromatography in a HisTrap HP column (Cytiva) equilibrated in buffer A on an ÄKTA Star system (Cytiva). Proteins were eluted by a continuous imidazole gradient of up to 500 mM imidazole in buffer A. The fractions containing the purified protein were pooled and concentrated by centrifugation at 4°C with an Amicon Ultra Centrifugal Filter Device with 50 000 MWCO (Millipore) and buffer exchanged to buffer B (25 mM Tris–HCl pH 7.5, 300 mM NaCl, 1 mM DTT and 10% (v/v) glycerol). Afterwards, the proteins were subjected to size exclusion chromatography using a Superdex 200 Increase 10/300 GL (Cytiva) and a flow rate of 0.5 mL/min using buffer B. Samples were collected and analyzed in Novex™ 4–12% Tris–glycine Mini Gels (Invitrogen) followed by BlueSafe staining (Nzytech, Portugal). Samples with the highest purity were pooled and concentrated by centrifugation at 4°C with an Amicon Ultra Centrifugal Filter device of 50 000 MWCO (Millipore). Proteins were quantified using the Bradford method and 50% (v/v) glycerol was added to the final fractions before storage at –20°C.

Activity assays

Exoribonucleolytic activity was assayed using two different RNA oligoribonucleotides as substrates. The 30-mer oligoribonucleotide (5′- CCCGACACCAACCACU AAAAAAAAAAAAAA-3′) and the poly(A) chain of 30 nt were labeled at their 5′-ends with [γ-^{32}P] ATP and T4 polynucleotide kinase (PNK) at 37°C for 1 h. The PNK was inactivated at 80°C for 5 min and the RNA oligomers were purified using a G25 column (Cytiva) to remove nonincorporated nucleotides. The labelled 30-mer oligoribonucleotide was hybridized to a complementary 16-mer oligoribonucleotide (5′- AGUGGUUGGUGUCGGG-3′) to obtain the corresponding 16–30 dsRNA. The hybridization was performed in a 1:2 (mol:mol) ratio in water for 5 min at 80°C, followed by 60 min incubation at 37°C. The exoribonucleolytic activity tests were carried out in a final volume of 15 μl containing 25 nM RNA substrate, 20 mM Tris–HCl pH 8, 100 mM KCl, 1 mM MgCl_2 and 1 mM DTT (when assessing the activity of RNase R alone) or 20 mM HEPES pH 7.4, 5 mM MgCl_2, 75 mM NaCl, 5

mM ATP and 1 mM DTT (when assessing the activity of RNase R with or without RhpA). The amount of each enzyme added to the mixture is indicated in each figure. Reactions were started by the addition of the enzyme followed by incubation at 37°C. Samples were taken at the indicated time points, and the reactions were stopped by addition of a formamide-containing dye supplemented with 10 mM EDTA. Reaction products were resolved in a 20% polyacrylamide/7 M urea gel and analysed by PhosphorImaging (FLA-2000, Fuji, Stamford, CT, USA).

Electrophoretic mobility shift assay (EMSA)

EMSAs were performed with the poly(A) substrate previously described in a final volume of 10 μl. Mixtures containing increasing enzyme concentrations (from 10 to 1000 nM), 25 nM poly(A) and binding buffer (10 mM Tris–HCl pH 8, 100 mM KCl, 25 mM EDTA and 2 mM DTT) were incubated for 10 min at 37°C. The reactions were stopped by adding 2 μl of loading buffer [30% (v/v) glycerol, 0.25% (w/v) xylene cyanole and 0.25% (w/v) bromophenol blue]. The RNA–protein complexes were subjected to ultraviolet fixation in a Cross-Linker. Samples were analyzed in a 6% non-denaturing polyacrylamide gel. The RNA–protein complexes were detected by PhosphorImaging (FLA-2000, Fuji, Stamford, CT, USA).

Helicase activity tests

To determine the helicase activity, we used a 16-base paired duplex with a 14-nt overhang (16-30ds), prepared as described in the previous section. The helicase activity tests were carried out in a final volume of 10 μl containing 10 nM of 16–30ds, and different buffer combinations (detailed in Supplementary Materials and Methods). The amount of each enzyme added to the reaction is indicated in the respective figures. Reactions were started by the addition of the enzyme and the mixtures were incubated at 37°C for 45 min. The reaction was stopped by adding a stop solution with 100 mM EDTA, 1% (w/v) SDS, 15% (v/v) glycerol, 0.25% (w/v) xylene cyanole and 0.25% bromophenol blue and 1 μM non-labeled 30-mer (to prevent the reannealing of the substrate). Reaction products were analyzed in a 20% polyacrylamide non-denaturing gel and analyzed by PhosphorImaging (FLA-2000, Fuji, Stamford, CT, USA).

Bacterial two hybrid

Bacterial two hybrid assays were carried out in *E. coli* strain BTH101 as previously described (58). Briefly, strains carrying derivatives of the two vectors, pUT18C and pKNT25, were grown overnight in 1 ml LB with 40 μg/ml kanamycin, 100 μg/ml ampicillin and 0.1 mM IPTG, and the resulting cultures were used for the measurements.

The OD at 600 nm of the resulting cultures was measured in a TECAN plate reader and the beta-galactosidase activity was calculated by mixing 500 μl of the cultures with 500 μl of buffer Z, 100 μl of chloramphenicol and 50 μl of 0.1% SDS, vortexing the cells and then adding 200 μl of 4 mg/ml ONPG. The reactions were incubated at 28°C until they turned yellow and the reactions were stopped by

adding 500 μl of 1 M Na_2CO_3. Samples were centrifuged for 5 min at 14 000 rpm and the OD at 420 and 550 nm of the upper fraction was measured in a TECAN plate reader. The beta-galactosidase activity (Miller units) was calculated as previously defined (59). The experiments were reproduced twice with eight replicates each time.

Affinity purification and mass spectrometry (AP-MS)

The complete procedure including sample preparation, affinity purification, liquid chromatography and mass spectrometry (LC–MS) acquisition as well as bioinformatic analyses are available in supplementary materials and methods.

Analytical ultracentrifugation

Purified protein samples were thawed on ice and the buffer was replaced using G-25 columns (PD MiniTrap G-25, GE Healthcare) with 25 mM Tris–HCl pH 8, 300 mM NaCl and 0.5 mM Tris(2-carboxyethyl)phosphine (TCEP, Sigma). Appropriate amounts of the different proteins were mixed and diluted in the same buffer with a final volume of 300 μl that was charged into two sector analytical ultracentrifugation cells. The centrifugation was performed for 16 h in an Optima analytical ultracentrifuge (Beckman-Coulter) with an 8-hole AnTi50 rotor, at 42 000 rpm and 20°C, measuring the optical density at 280 nm in order to determine the sedimentation profile of the protein or complex. The data were analyzed with the SedFit software (NIH) using a diffusion deconvoluted continuous sedimentation coefficient distribution $c(s)$ model with one discrete species (60).

The partial specific volume (V_{bar}) of the proteins was estimated by the software Sednterp (61) based on the amino acid sequence. This software was also used for the calculation of the density and viscosity of the buffer used throughout the experiments. The experiments were reproduced two times and produced identical results.

Surface plasmon resonance (SPR)

Surface plasmon resonance was performed by using a CM5 sensor chip (Cytiva) and a Biacore 2000 system (Cytiva). Purified *Hp*RNase R was immobilized in flow cell 2 of the CM5 sensor chip by the amine coupling procedure. The surface was activated with a 1:1 mixture of 1-ethyl-3-(3-dimethylaminopropyl) carbodiimide (EDC) and *N*-hydroxysuccinimide (NHS) and injected for 5 min at a flow rate of 10 μl/min. Then, 20 μg of *Hp*RNase R were injected during 10 min at the same flow rate. After injection of the ligand, ethanolamine was injected to the surface in order to deactivate it. The immobilization of the protein originated a response of 144 RU. On flow cell 1, BSA protein was immobilized using the same method and this cell was used as a control. Biosensor assays were run at 15°C in a buffer with 25 mM Tris pH 7.5, 300 mM NaCl and 1 mM DTT. Serial dilutions of purified RhpA were injected over flow cells 2-1 for 3 min at different concentrations using a flow rate of 20 ml/min. The dissociation was allowed to occur during 5 min in the running buffer. All experiments included triple injections of each protein concentration to determine signal

reproducibility. Bound proteins were removed after each cycle with a 30 s wash with 2 M NaCl. After each cycle, the signal was stabilized for 1 min before a new protein injection. Data from flow cell 1 was used to correct for refractive index changes and nonspecific binding. Rate constants were calculated using the BIAEVALUATION 3.0 software package by fitting the sensograms obtained to a 1.1 Langmuir binding model. K_D was calculated as the ratio between k_d and k_a.

Cellular fractionation of *H. pylori*

We used the protocol as described in (11). Briefly, *H. pylori* cells were grown to an $OD_{600 nm}$ of 0.7–1, harvested by centrifugation, resuspended in 10 mM Tris–HCl pH 7.4 and cOmplete Protease Inhibitor cocktail (Roche) (buffer A) to an $OD_{600 nm}$ of 5. Bacteria were disrupted by sonication. Cell debris was removed by centrifugation and supernatants were collected as total extracts. The supernatants were centrifuged 45 min at 100 000g at 4°C in a TLA-100 ultracentrifuge (Beckman Coulter) using a TLA-55 rotor and supernatants were collected as soluble extracts. The pellet was resuspended in buffer A + 0.1% SDS (Sigma-Aldrich) (buffer B). After another ultracentrifugation under the same conditions, the supernatant contains the inner membrane and the pellet the outer membrane.

Western blotting

Proteins were loaded and separated on a 4–20% Mini-Protean TGX Stain-Free precast protein gel (Biorad) and transferred to a nitrocellulose membrane (iBlot™ Transfer Stack, Thermo Fisher Scientific) with the iBlot2™ Gel Transfer Device (Thermo Fisher Scientific). The *H. pylori* RhpA and AmiE proteins were detected with rabbit polyclonal antibodies α-RhpA (2) and α-AmiE (62) at 1:5000 and 1:500 dilutions, respectively. RNase R-HA was detected with rabbit α-HA antibodies (Sigma) at 1:10 000 dilution. Goat anti-rabbit IgG-HRP (Santa Cruz) was used as secondary antibody at 1:10 000 dilution and detection was achieved with the ECL Plus reagent (Thermo Fisher). Images were taken with a ChemiDoc MP Imaging System (BioRad).

RNA extraction and sequencing

RNA was extracted from 2 ml *H. pylori* cultures at an $OD_{600 nm}$ of 0.5 in Brucella medium using a Total RNA Purification kit (Norgen Biotek Corp) and the samples were stored at –80°C until further processing. RNA was prepared in triplicates from three independent cultures for each strain (WT, *ΔrhpA* and *Δrnr*).

The QIAseq Fast Select –5S/16S/23S (QIAGEN) kit was used for ribosomal RNA depletion according to manufacturer instructions. Libraries were built using a TruSeq Stranded mRNA library Preparation Kit (Illumina, USA) following the supplier's recommendations. Quality control was performed on an Agilent Bioanalyzer. RNA sequencing was performed on the Illumina NextSeq 500 platform using single-end 75 bp.

RNA-seq analysis

The RNA-seq analysis was performed with Sequana 0.8.0 (63). In particular, we used the RNA-seq pipeline (v0.9.16, https://github.com/sequana/sequana_rnaseq) built on top of Snakemake 5.8.1 (64). Reads were trimmed from adapters using Cutadapt 2.10 (65) then mapped to the *H. pylori* B8 (NC_014256.1) genome assembly from NCBI using Bowtie 2.3.5 (66). FeatureCounts 2.0.0 (67) was used to produce the count matrix, assigning reads to features using annotation from NCBI NC_014256.1 with strand-specificity information. Quality control statistics were summarized using MultiQC 1.8 (68). Statistical analysis on the count matrix was performed to identify differentially regulated genes, comparing wild type *H. pylori* strain to the Δrnr and $\Delta rhpA$ mutants and Δrnr and $\Delta rhpA$ strains to each other. Clustering of transcriptomic profiles were assessed using a principal component analysis (PCA). Differential expression testing was conducted using DESeq2 library 1.24.0 (69) scripts based on SARTools 1.7.0 (70) indicating the significance (Benjamini–Hochberg adjusted *P*-values, false discovery rate FDR < 0.05) and the effect size (fold-change) for each comparison. Differentially-regulated genes are listed in Supplementary Table S3.

3′-Rapid amplification of cDNA ends (3′-RACE)

Total RNA was treated with poly(A) polymerase (NEB) following the supplier's recommendations. 3′-RACE was performed using the 3′ RACE System for Rapid Amplification of cDNA Ends (Thermofisher). Total poly(A) RNA was reverse transcribed and used for PCR amplification of the cDNA molecules that correspond to the 23S, 16S or 5S rRNAs and *tm*RNA using the primers described in Supplementary Table S2 and an oligo dT supplied with the kit. The resulting fragments were cloned into the pGEM-T Easy system (Promega) and blue/white colony screening was performed on LB plates containing 100 μg/ml ampicillin, 1 mM IPTG and 20 μg/ml X-Gal (5-bromo-4-chloro-3-indolyl-ß-D-galactopyranoside). The fragments cloned in the pGEM-T multicloning site of 10 individual white colonies for each gene of interest were PCR amplified and sequenced (Eurofins Genomics).

Statistical analysis

The statistical analysis performed in the two hybrid experiments were carried out on Prism v 9, using one-way ANOVA with Tukey's multiple comparison test.

RESULTS

Progressive loss of helicase signature motifs in RNase R from the *Campylobacterota*, a phylum including *Helicobacter pylori* and *Campylobacter jejuni*

The RNB family is composed of both RNase R and RNase II proteins. In *H. pylori*, only one gene, *rnr*, was identified as encoding a protein of this family. It was predicted to code for an RNase R protein and its 3′-5′ exoribonuclease activity was demonstrated (41). First, we aligned *Hp*RNase R

with its orthologs from *E. coli* and the closely related organism *C. jejuni*, and with RNase II from *E. coli* (Supplementary Figure S1). This analysis revealed that the RNase R proteins from *H. pylori* and *C. jejuni* are similar and are more closely related to *Ec*RNase R than to *Ec*RNase II, validating that they are indeed orthologs of *Ec*RNase R. In addition, we observed that both *Hp*RNase R and *Cj*RNase R lack several regions that have, in *Ec*RNase R, been associated with its helicase function, including the Walker A and B motifs that are important for ATP binding (Figure 1A and Supplementary Figure S1). Specifically, in *Ec*RNase R, the Walker A motif, located in a region downstream from the S1 domain, is absent in *Hp*RNase R and *Cj*RNase R. In addition, the Walker B motif of *Ec*RNase R is located at the beginning of the CSD2 domain in a region that is also absent from both *Hp*RNase R and *Cj*RNase R. In these two latter organisms, the S1 domain, important for dsRNA binding, is truncated, the two CSD regions are degenerated, in particular in *H. pylori*, and the basic C-terminal domain is absent. Moreover, the tri-helix region within the RNB domain, which was found to be crucial for RNA unwinding in *Ec*RNase R, is not conserved in *Hp*RNase R and *Cj*RNase R.

Next, we performed a phylogenetic analysis to determine whether this domain organization and deletions correspond to a common feature of the RNase R proteins of the *Campylobacterota* phylum. A set of 322 reference genomes (including *H. pylori* and *C. jejuni*) was retrieved from the Genome Taxonomy Database (GTDB) (50) and was used to create a phylogenetic tree (Figure 1B and Supplementary Figure S2), where the different families of *Campylobacterota* are clearly distinguished by a strong branch support. We identified 297 RNase R protein candidates from these genomes by the presence of a core domain characterized by the PF00773 profile. We validated that these proteins are indeed orthologs of RNase R and not RNase II using the sequences of the *E. coli* proteins as a reference (Supplementary Figure S3). As no RNase R/II homologues were found in 29 of these genomes, *tblastn* was used to search in DNA sequences for the presence of a region of similarity with *Ec*RNase R but whose corresponding gene would not have been correctly predicted. This allowed us to identify orthologs in six additional genomes. The remaining 23 genomes do not possess an RNase R/II encoding gene, as is the case in the 11 complete genomes of the recently assigned genus *Helicobacter* E from GTDB, or this gene is missing because the genomes are not complete.

Using Pfam annotation, we observed that the RNB domain is very well preserved in all proteins. The first CSD (annotated by the Pfam OB_RNB or CSD2 profiles) is the best preserved, especially in *Campylobacteraceae* (Figure 1B). A lower prevalence of this latter domain is found in the *Arcobacteraceae* and especially in the *Helicobacteraceae*, notably in those that diverged more recently (including *H. pylori*, Figure 1B and Supplementary Figure S2). An intact S1 domain can only be found in the *Hippeaceae* and *Desulfurellaceae* genomes, which diverged first, suggesting that the S1 domain would have been lost in the other *Campylobacterota*. Our observations suggest that, during the course of evolution, there was a progressive degeneration of the CSD domains in the *Campylobacterota*, with

an acceleration in the *Helicobacteraceae*. Within this family, the genus *Helicobacter E* (including *H. suis*, *H. heilmannii*, *H. ailurogastricus*, *H. bizzozeronii* and *H. felis*) is the most extreme, as these genomes have lost the gene coding for RNase R.

Thus, the domains responsible for the helicase activity of *Ec*RNase R are poorly conserved across the RNase R proteins of the *Campylobacterota* and seem to have been lost in a progressive manner during evolution up to the *Helicobacteraceae*.

H. pylori **RNase R displays 3′-5′ exoribonuclease activity but does not act as a helicase**

To test our hypothesis that *Hp*RNase R is devoid of helicase activity, we overexpressed and purified recombinant *Hp*RNase R and the catalytic mutant D231N, which lacks ribonucleolytic activity (41) but, based on the sequence, should retain its ability to bind RNA. We used purified *Ec*RNase R as a control. As expected, on a single stranded poly(A) RNA substrate, *Hp*RNase R presents 3′-5′ exoribonuclease activity releasing 2 and 4 nucleotides (nt) fragments as end products (Figure 2A), similarly to what we observed and was reported for the *E. coli* protein (57). As expected, the *Hp*RNase R D231N mutant was unable to cleave the Poly(A) substrate (Figure 2A), although it was able to bind RNA as efficiently as the wild type protein (Figure 2B). We then tested whether *Hp*RNase R is able to degrade a partially double-stranded RNA substrate (16-30ds) that contains a 14 nt single-stranded overhang. While *Ec*RNase R was able to efficiently degrade this substrate, *Hp*RNase R only presented a residual activity even in the presence of 5 times more protein (Figure 2A). Once again, the D231N mutant was inactive on this substrate (Figure 2A). Considering the poor efficiency of *Hp*RNase R in cleaving dsRNA and our bioinformatic domain analysis, we speculated that this protein does not possess a helicase activity. To test this, we carried out a helicase activity assay as previously published (29) using the 16–30ds RNA molecule and 2.5 μM of the exoribonucleolytically inactive *Hp*RNase R D231N mutant. We tested 8 different buffer conditions (B1-B8, detailed in the legend of Figure 2C) and no helicase activity was detected for *Hp*RNase R (Figure 2C).

Altogether, our data clearly demonstrate that *Hp*RNase R has no helicase activity *in vitro* under these assay conditions.

*Hp*RNase R interacts with the RhpA DEAD-box RNA helicase

The genome of *H. pylori* expresses only one DEAD-box RNA helicase, RhpA (10), which we showed to be associated with RNase J as part of an RNA degradosome (2). Because *Hp*RNase R is devoid of helicase activity, we wondered whether this protein might interact with the RhpA helicase. Therefore, we performed bacterial two hybrid (BACTH) experiments in *E. coli*, expressing RhpA and *Hp*RNase R fused to different subunits of adenylate cyclase (T25 and T18) and measuring ß-galactosidase activity. We

found that, when RhpA was fused at the N-terminus of T25 and RNase R was fused at the C-terminus of T18, a positive interaction could be detected (Figure 3A).

Then, we investigated the RhpA-*Hp*RNase R complex formation *in vitro*. We also overexpressed and purified recombinant RhpA and performed analytical ultracentrifugation (AUC) at 280 nm wavelength. We observed that *Hp*RNase R alone behaves as a monomer *in vitro* independently of the protein concentration with a sedimentation coefficient of ∼4.25S (Figure 3B). After addition of RhpA in a 5:1 RhpA:*Hp*RNase R proportion, we followed the sedimentation of *Hp*RNase R at 280 nm, as RhpA does not absorb at this wavelength due to its lack of aromatic amino acids. Under this condition, a new peak with a sedimentation coefficient of about 5S appears as well as a smaller peak with a sedimentation coefficient of about 10S (Figure 3C). The increase in the sedimentation coefficient of the major peak is only consistent with the formation of a 1:1 stoichiometry complex. Thus, *Hp*RNase R and RhpA form a stoichiometric complex in solution.

To further characterize their interaction, we performed a surface plasmon resonance (SPR) analysis to determine the *in vitro* affinity of *Hp*RNase R with its partner RhpA (Figure 3D). Purified *Hp*RNase R was immobilized on a sensor chip, increasing concentrations of purified RhpA were injected and the response was monitored. The results presented in Figure 3D further confirm the interaction between RhpA and *Hp*RNase R and allowed us to determine an affinity constant (K_D) of 29 ± 4.4 nM. Furthermore, we measured the kinetic constants of this interaction and found an association constant (k_a) of $3.5 ± 0.3 × 10^4$ (M·s)$^{-1}$ and a dissociation constant (k_d) of $1.0 ± 0.1 × 10^{-3}$ s^{-1}.

To validate the existence of this complex in *H. pylori* cells, an *H. pylori* strain expressing, from its native locus, an *Hp*RNaseR protein tagged with an HA epitope at its C-terminus was used for affinity purification and mass spectrometry (AP-MS) experiments using anti-HA antibodies. We observed that, indeed, RhpA is an interacting partner of *Hp*RNase R in *H. pylori* cells, along with other proteins such as ribosomal proteins (Supplementary Figure S4 and Table S4).

Altogether, our data demonstrate that *Hp*RNase R and RhpA form a complex in *H. pylori*.

Formation of the RhpA-*Hp*RNase R complex stimulates exoribonuclease activity on dsRNA *in vitro*

In order to study the consequences of the RhpA-*Hp*RNase R complex formation on the degradation of dsRNA, we tested the exoribonucleolytic activity of *Hp*RNase R in the presence of RhpA *in vitro*. First, we tested different buffers (B1-B8) to determine the optimal conditions for RhpA to display helicase activity *in vitro* (Figure 4A). RhpA presents helicase activity under several conditions, of which we chose buffer B5 for the following experiments. As shown in Figure 4B, *Hp*RNase R alone is not efficient in the degradation of dsRNA, and no degradation is observed upon incubation of the dsRNA substrate with RhpA alone. When both enzymes were mixed together at the same concentration, a slight disappearance of the intact dsRNA substrate was
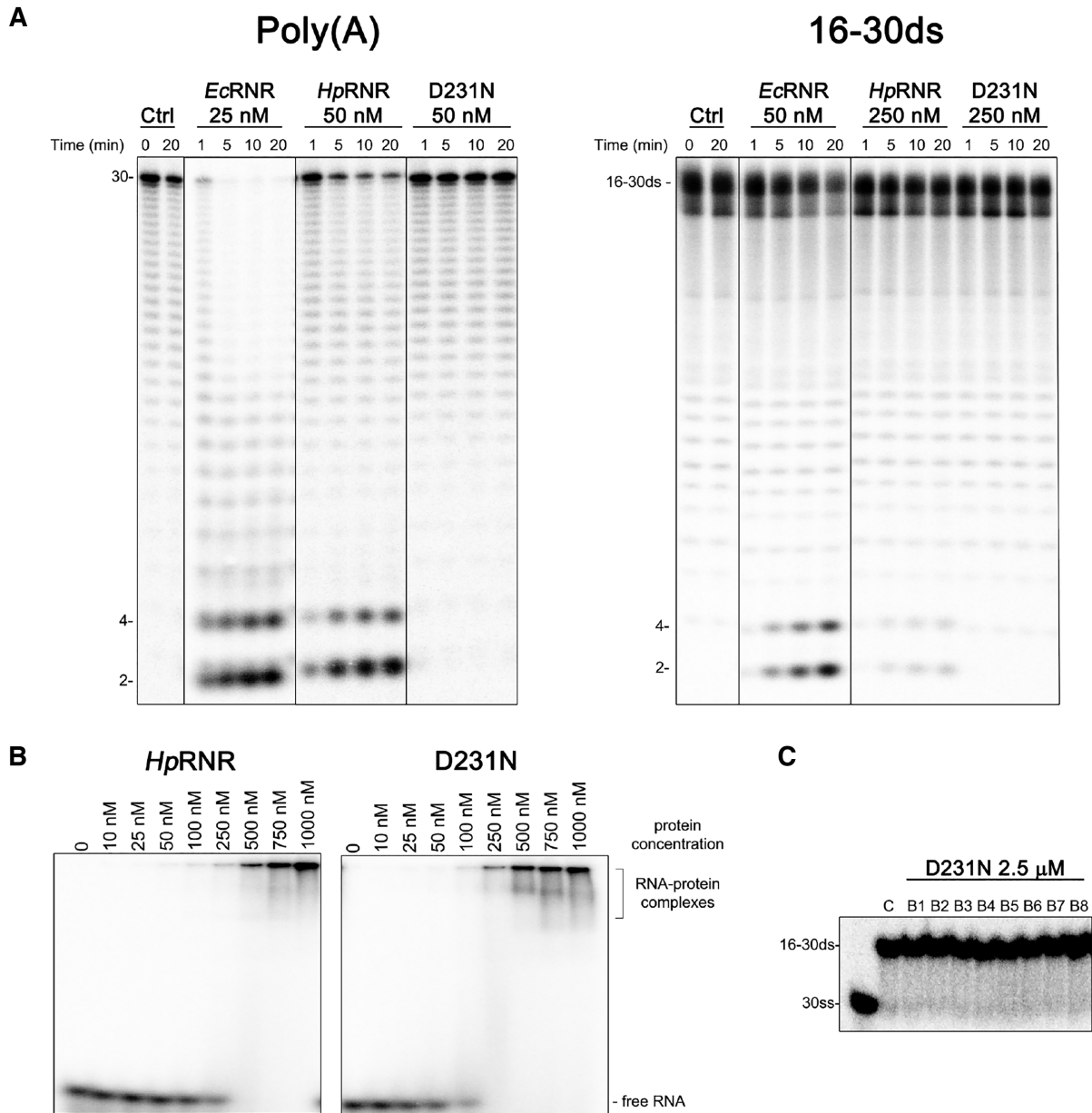
Figure 2. *In vitro*, *Hp*RNase R displays 3′-5′ exoribonuclease activity but no helicase activity. (**A**) 3′-5′ exoribonuclease activity tests over 20 min, of *Ec*RNases R and *Hp*RNase R on a poly(A) ssRNA substrate (left panel) or on a 16–30ds partially dsRNA substrate (right panel). The catalytically inactive *Hp*RNase R D231N mutant served as a control. The end-products are indicated as we previously reported (79). (**B**) Electrophoretic mobility shift assay (EMSA) of wild type *Hp*RNase R and the *Hp*RNase R D231N mutant. (**C**) Helicase activity assay of the catalytically inactive *Hp*RNase R D231N mutant using eight different buffers B1 to B8. B1: 50 mM Tris–HCl pH 7.5, 5 mM ATP, 50 mM MgCl$_2$, and 20 mM NaCl; B2: 50 mM Tris–HCl pH 7.5, 5 mM ATP, 5 mM MgCl$_2$ and 50 mM NaCl; B3: 20 mM Tris–HCl pH 7.5, 5 mM ATP, 5 mM MgCl$_2$ and 75 mM NaCl; B4: 20 mM Tris-HCl pH 7.5, 5 mM ATP, 5 mM MgCl2, 75 mM NaCl and 1mM DTT; B5: 10 mM HEPES pH 7.4, 5 mM ATP, 5 mM MgCl$_2$, 75 mM NaCl and 1 mM DTT; B6: 10 mM HEPES pH 7.4, 5 mM ATP, 5 mM MgCl$_2$ and 75 mM NaCl; B7: 20 mM HEPES pH 7.4, 5 mM ATP, 5 mM MgCl$_2$, 75 mM NaCl and 1 mM DTT; B8: 10 mM HEPES pH 7.4, 5 mM ATP, 5 mM MgCl$_2$, 50 mM NaCl and 1 mM DTT.

detected, which suggests that RhpA facilitates the degradation of structured RNAs by *Hp*RNase R. We next copurified both enzymes from *E. coli*, by mixing the pellets overexpressing each protein before cell lysis and protein purification, and tested their ribonucleolytic activity. Interestingly, this condition was found to be much more active and to completely degrade the initial dsRNA substrate to 8–15

end-products in 10 min (Figure 4B). We speculate that, under these conditions, the interaction of *Hp*RNase R with RhpA limits the access of smaller RNA molecules to the *Hp*RNase R active site, resulting in the larger degradation products (8–15 nt) observed in Figure 4B as compared to the 2–4 nt products observed with *Hp*RNase R alone in Figure 2A.
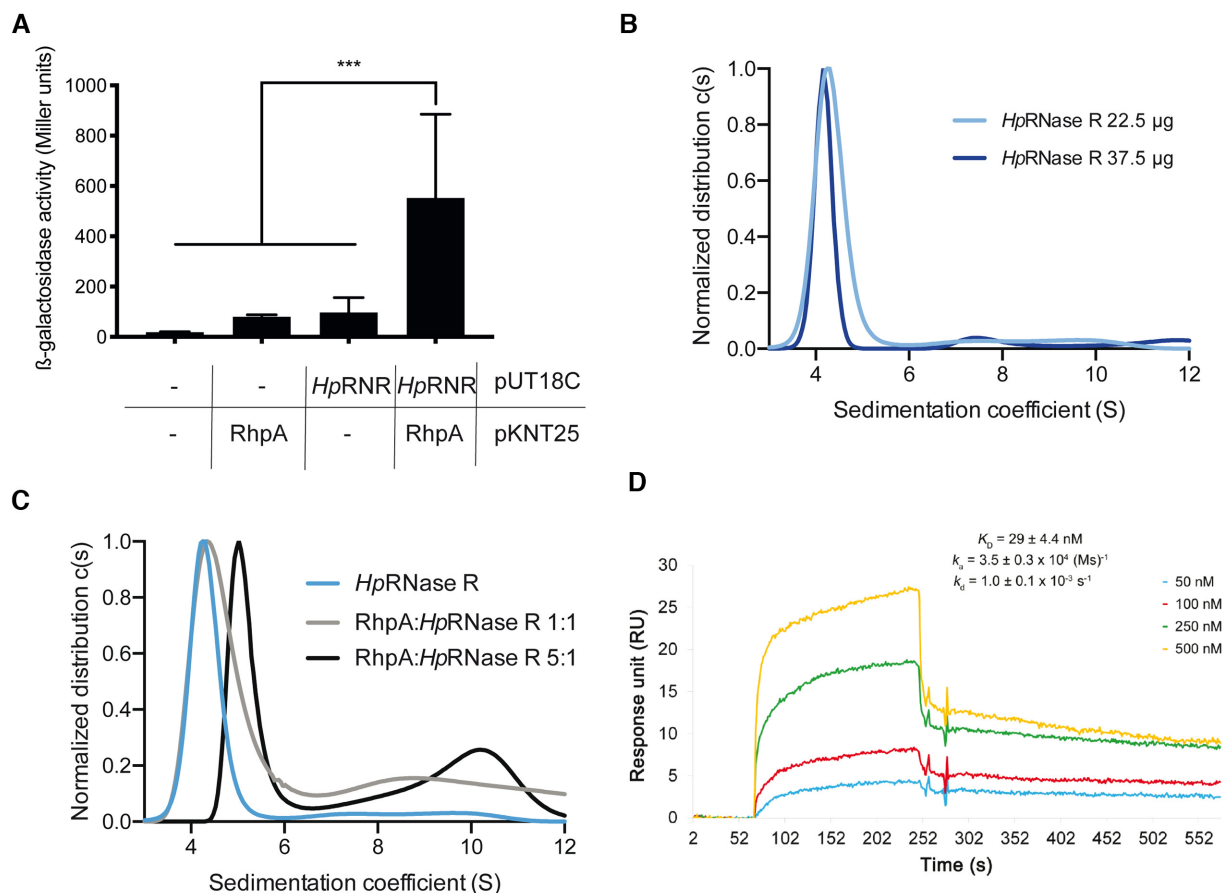
Figure 3. *Hp*RNase R interacts with the DEAD-box RNA helicase RhpA. (**A**) Beta-galactosidase activity from a bacterial two hybrid assay testing the interaction between *Hp*RNase R and RhpA. *** indicates a *P*-value <0.0001. (**B**) Sedimentation profile at 280 nm of *Hp*RNase R obtained by analytical ultracentrifugation. (**C**) Sedimentation profile at 280 nm of the *Hp*RNase R-RhpA complex obtained by analytical ultracentrifugation. (**D**) The interaction between *Hp*RNase R and RhpA was measured by surface plasmon resonance assay (SPR), the different lines correspond to different RhpA concentrations indicated on the figure. The K_D affinity constant was calculated as the ratio between k_d and k_a values.

These results demonstrate that *Hp*RNase R and RhpA form a functional complex with an increased exoribonuclease activity of *Hp*RNase R on dsRNA substrates *in vitro*.

*Hp*RNase R is associated with the inner membrane of *H. pylori*, independently of RhpA

We recently reported that the two partners of the RNA degradosome, RhpA and RNase J, localize to the inner membrane of *H. pylori* (11). Just like RhpA and RNase J, the *Hp*RNase R protein does not present any transmembrane segment or signal peptide (Supplementary Figure S5). We also examined whether *Hp*RNase R possesses an amphipathic helix that could account for membrane association similarly to *Ec*RNase E and *Ec*RNase II. Although such a helix can be predicted in the N-terminus of RNase R from some *H. pylori* strains, the corresponding sequence is not conserved among the analyzed strains. The cellular localization of *Hp*RNase R was tested using cellular fractionation of the *H. pylori* strain expressing *Hp*RNase R-HA from its native locus. Western blot analysis of the different fractions revealed that *Hp*RNase R-HA mainly localizes at the inner membrane independently of RhpA (Figure 5). More work is needed to define the membrane anchor of

*Hp*RNase R. This further shows that, in *H. pylori*, several proteins involved in RNA degradation localize to the inner membrane, suggesting a compartmentalization of these functions.

*Hp*RNase R has a restricted number of RNA targets that are shared with the RhpA helicase

*Hp*RNase R is not essential in *H. pylori*. Indeed the *Δrnr* mutant is viable, only slightly affected in growth (Supplementary Figure S6A) and not deficient in motility in contrast to the noticeable growth defect and reduced motility that we found for a *ΔrhpA* mutant (10). In order to define the *Hp*RNase R RNA targets in *H. pylori*, we first assessed whether its expression is regulated as it has been reported in *E. coli*. The expression of RNase R seems constitutive in *H. pylori* since the amounts of *Hp*RNase R-HA protein are not affected by growth phase, not induced during growth at lower temperature (33°C, the lowest temperature at which *H. pylori* grows) or upon overnight exposure to 4°C (Supplementary Figure S6B, C).

RNA-Seq was thus performed to define the global transcriptome changes of a *Δrnr* mutant in exponential phase as compared to a wild type strain. For comparison, we also
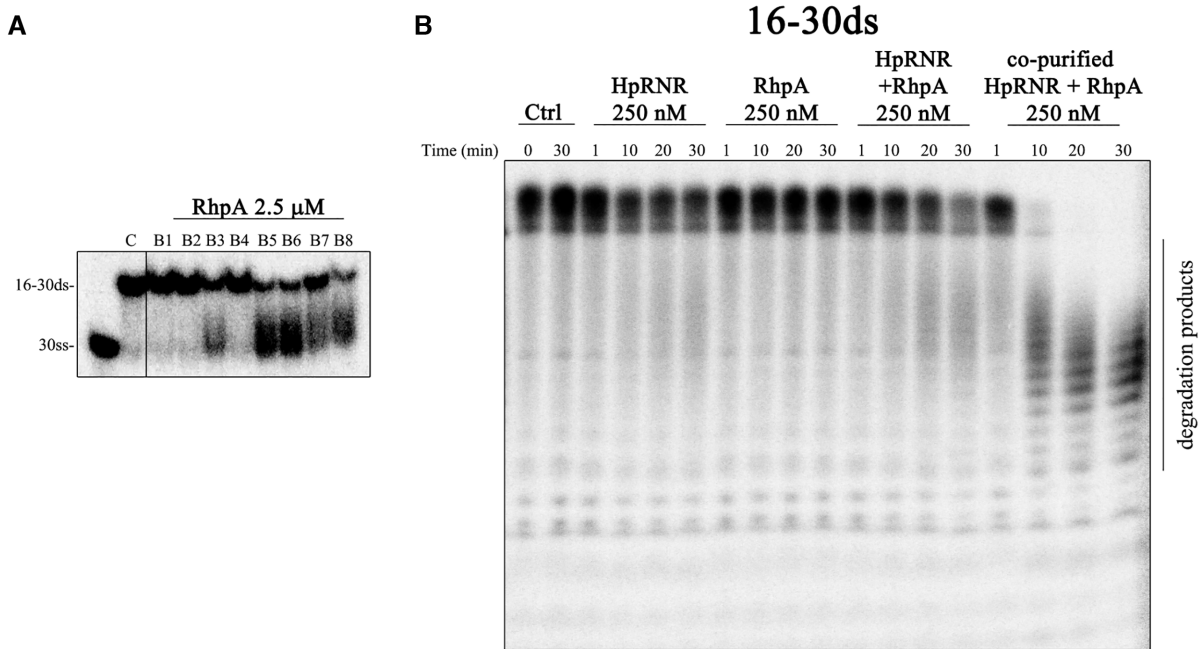
A

B

16-30ds

Figure 4. *Hp*RNase R and RhpA form a functional complex *in vitro*. (**A**) RhpA helicase activity was tested with 8 different buffers (B1 to B8) and helicase activity on a 16–30ds RNA substrate was detected in 5 of the tested conditions. (**B**) 3′-5′ exoribonuclease activity test, during 30 min, on a 16–30ds RNA substrate with *Hp*RNase R or RhpA alone or both proteins in complex (reconstituted or co-purified). Degradation of the substrate is strongly accelerated when both proteins are copurified.
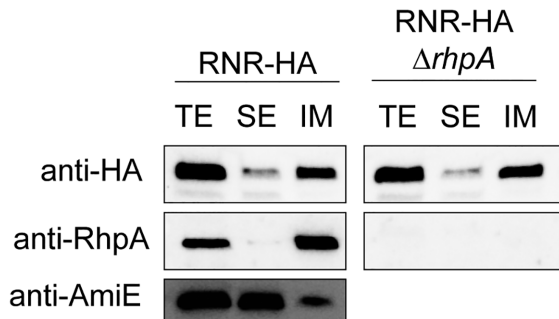
Figure 5. *Hp*RNase R-HA localizes to the inner membrane independently of RhpA. Western blot carried out with samples resulting from a subcellular fractionation of *H. pylori* strains expressing an HA-tagged version of *Hp*RNase R from its native locus on the chromosome in a wild type context or in a *ΔrhpA* mutant. TE, total extract; SE, soluble extract; IM, inner membrane.

Figure 6. Venn diagram showing the overlap of differentially expressed genes between the transcriptomes of the *H. pylori* wild type, *ΔrhpA* and *Δrnr* strains.

performed RNA-Seq of the *ΔrhpA* mutant. We observed that, in the *Δrnr* strain, there were very few RNAs whose amount was significantly changed (only 11), with 5 being downregulated (one of them being the deleted *rnr* gene itself) and 6 being upregulated, including mRNAs and a few asRNAs (Supplementary Table S3). Among the upregulated transcripts, we found the mRNAs coding for LpxC, an enzyme important for lipopolysaccharide biosynthesis, and Dcm1, a predicted methyltransferase. A list of the differentially expressed genes in the *Δrnr* mutant together with the validation of the changes by qRT-PCR can be found in Supplementary Tables S3 and S5.

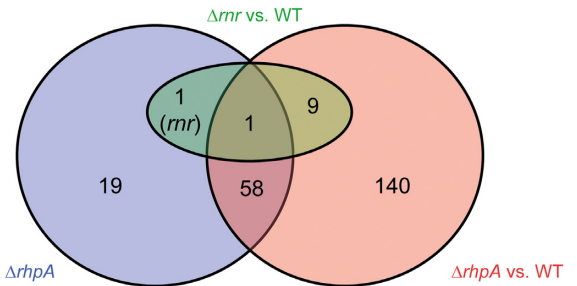In contrast to the *Δrnr* strain, the *ΔrhpA* strain shows more dramatic changes at the transcriptome level, with 208 differentially regulated genes with respect to the wild type strain, 90 of which being downregulated (63 mRNAs and 27 sRNAs and asRNAs) and 118 upregulated (114 mRNAs and 4 asRNAs). A list of all differentially regulated genes in the *ΔrhpA* strain can be found in Supplementary Table S3. When we compared the transcriptomes of the *Δrnr* and *ΔrhpA* strains, we found a total of 79 differentially-regulated genes, 58 of which are also differentially expressed when WT is compared to the *ΔrhpA* mutant, further suggesting that the *Δrnr* strain does not have many specific targets, and only 20 genes being exclusively differentially expressed between the *Δrnr* and *ΔrhpA* strains. Importantly, every potential target of *Hp*RNase R (green circle in Figure 6) is similarly dysregulated in both *Δrnr* and *ΔrhpA* mutant strains (Figure 6 and Supplementary Table S5), with the exception of the *hpb8_899* gene encoding a protein of unknown function, that is considerably less expressed in the

Table 1. Percentages of the 3′-end species of the 23S, 16S and 5S rRNAs and *tm*RNA, sequenced by 3′-RACE, in the B128, Δ*rhpA* and Δ*rnr* strains

3′-end species	% sequences		
	B128	Δ*rhpA*	Δ*rnr*
23S rRNA annotation: 5′-… TTGTTTTT-3′			
–3 nt	11	25	17
–2 nt	22	25	50
–1 nt	22	25	-
+1 nt	22	-	17
+47 nt	-	-	17
+50 nt	22	25	-
16S rRNA annotation: 5′-…TCACCTCCT-3′			
–11 nt	-	-	12
+2 nt	-	13	-
+3 nt	89	62	88
+4 nt	11	-	-
+79 nt	-	25	-
5S rRNA annotation: 5′-…ATAGGGAAAT-3′			
–7–8 nt	83	86	67
–6 nt	-	-	11
–5 nt	-	14	11
–1–4 nt	17	-	-
+1 nt	-	-	11
*tm*RNA annotation: 5′-…GCTCCACCA-3′			
–2 nt	-	17	-
–1–0 nt	100	83	100

Highlighted in blue are the species whose amount is decreased and in orange are the species whose amount is increased. In the first column, the length of the 3′-ends of the sequenced cDNA molecules is expressed as compared to the annotated 3′ end (e.g. –3 nt indicates that the sequenced molecule is 3 nt shorter than the annotation and +47 nt indicates that the sequenced molecule is 47 nt longer).

Δ*rnr* strain than in the Δ*rhpA* strain and the deleted *rnr* gene itself.

We concluded that *Hp*RNase R alone plays a minor role in the control of the stability of RNAs in exponential phase growing *H. pylori* and that this activity most probably requires RhpA.

Minor role of *Hp*RNase R in the 5S rRNA maturation

In *E. coli*, RNase R has been reported to play an important role in the maturation of rRNAs and the functionality of *tm*RNA. In *H. pylori*, we previously reported a defect in the maturation of 16S rRNA in a Δ*rhpA* strain (10) and the essentiality of *tm*RNA (71). Therefore, we wondered whether *Hp*RNase R might also be important for the maturation of rRNAs or *tm*RNA in *H. pylori*. We performed 3′-Rapid Amplification of cDNA Ends (3′-RACE) sequencing on RNA extracted from wild type, Δ*rnr* and Δ*rhpA* strains in order to define the 3′-extremities of 5S, 16S and 23S rRNAs and *tm*RNA in these strains. As expected, the Δ*rhpA* strain presented a defect in the maturation of the 16S rRNA, with 25% of the sequences showing a long 79 nt-extended 3′-extremity (Table 1). The Δ*rhpA* strain presented no major defect in the maturation of the other rRNAs or of the *tm*RNA. The Δ*rnr* mutant presented no defect in *tm*RNA 3′-maturation. The mutant deficient in *Hp*RNase R only displayed a mild defect in 5S rRNA maturation, with 33% of the sequences having a slightly longer 3′-extremity (1-7 nt longer than the predominant species) (Table 1).

These data showed that, in *H. pylori*, RhpA is important for the 3′-end maturation of 16S rRNA independently of *Hp*RNase R and that this latter exoribonuclease has only a minor role in the maturation of 5S rRNA independently of RhpA.

RNase R and DEAD-box RNA helicases frequently co-occur in the *Campylobacterota*

We finally sought to define, in other members of the *Campylobacterota* phylum, the distribution of RNase R, DEAD-box RNA helicases and other prominent RNA degradation proteins, such as RNase J and PNPase. For that, we identified proteins from the DEAD-box (PF00270, here referred to as CsdA), RNase J (MF_01491) and PNPase (MF_01595) families and we summarized their frequencies in the strains by grouping them by taxonomic rank (Figure 7). We found that RNase J and PNPase proteins are present in all *Campylobacterota* families and that RNase R and DEAD-box proteins frequently co-occur, although there are some cases where one or the other is absent. For instance, the *Thiovulaceae* and the genus *Helicobacter E* lack RNase R, whereas the *Campylobacteraceae* lack CsdA-like proteins. Thus, with the exception of the *Campylobacteraceae* such as *C. jejuni*, which lack a DEAD box RNA helicase (10), the vast majority of the *Campylobacterota* presents a co-occurrence of RNase R and a DEAD-box RNA helicase, a situation that might be compatible with a conserved interaction between these two proteins.

DISCUSSION

The 3′-5′ exoribonuclease RNase R from *E. coli* has been shown to possess an additional helicase activity allowing this enzyme to act on partially structured RNA molecules. Here we demonstrated that this unwinding activity is not a general feature of the RNase R proteins. Studying the *H. pylori Hp*RNase R, we observed that the domains and motifs required for *Ec*RNase R helicase activity are not conserved in *H. pylori*. These motifs include the tri-helix wedge within the RNB domain, that contains the helicase activity *per se* (32), two Walker motifs present in the CSD2 and K/R-rich domains (29), responsible for ATP binding and hydrolysis, and residues important for dsRNA binding to the S1 domain (30). RNase R and RNase II are two closely related members of the RNB exoribonuclease family. Our bioinformatic analysis allowed us to unambiguously distinguish the RNase R proteins and thus to explore for the first time the evolution of their functional domains. Within the *Campylobacterota* phylum that includes *H. pylori*, the RNase R S1 domain is either absent or strongly degenerated and the CSD domains are poorly conserved. Our analysis points to the gradual loss of these domains over the course of evolution of the members of this phylum.

In vitro assays with purified *Hp*RNase R revealed a slightly lower 3′-5′ exoribonuclease activity as compared to *Ec*RNase R on fully single-stranded RNA substrates. Most importantly, we confirmed that *Hp*RNase R does not display helicase activity in the tested conditions and is unable to digest even partially double-stranded RNA substrates. We previously reported a very weak ribonuclease activity of
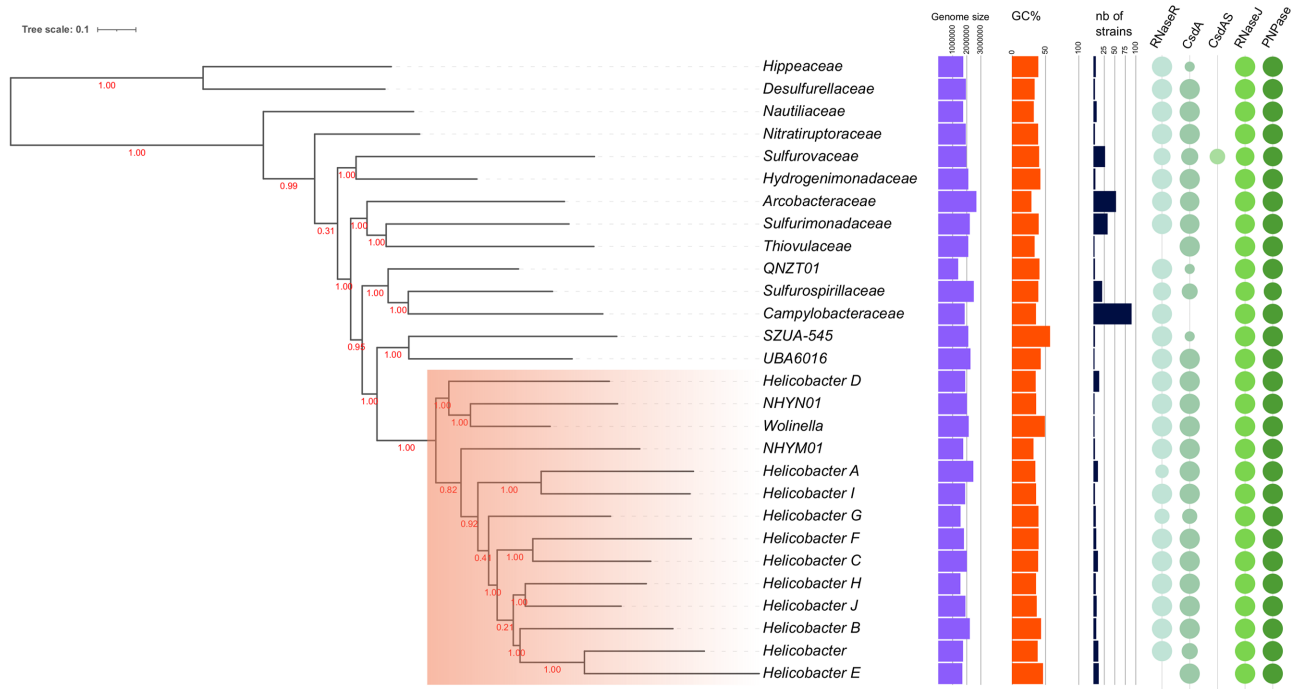
Figure 7. Taxonomic distribution of the protein families of RNases, RNase R, RNase J and PNPase and of the CsdA helicase. The phylogenetic tree has been pruned at the family rank except for the *Helicobacteraceae*, where it is at the genus level (orange shading). The average sizes of the genomes and their average G+C content is mentioned, as well as the number of genomes (strains) analyzed per family rank. The diameter of the circles is proportional to the percentage of homologous genes observed in the genomes clustered under each taxonomic rank. CsdAS refers to a group of CsdA paralogues that was found only in the *Sulfurovaceae*. The figure was made with *iTOL* v5.

*Cj*RNase R on a fully dsRNA substrate and a moderate activity with a double stranded RNA with 14-nt 3′-overhang (26). The difference between the *Hp*RNase R and *Cj*RNase R activities could be explained by a weak conservation of the CSD1 domain in the proteins of *Campylobacteraceae* to which *C. jejuni* belong. As can be seen in Supplementary Figure S1, the N-terminal extremity of the *Hp*RNase R CSD1 domain is strikingly degenerated as compared to those of *Cj*RNase R and *Ec*RNase R. We speculate that this region could be important for the binding of dsRNA sequences and that the *Cj*RNase R would therefore conserve some degradation activity on dsRNA with an overhang region. However, future experimental data are needed to validate this hypothesis. Interestingly, *Ec*RNase R deprived of its helicase activity (by mutations in the S1 domain or without added ATP) can also degrade structured RNAs with a 3′-overhang of at least 10 nt (30).

We demonstrated that *Hp*RNase R forms a complex with RhpA, the sole DEAD-box RNA helicase of *H. pylori*. This interaction was shown by several approaches; in live cells by *E. coli* BACTH and in *H. pylori* by affinity purification-mass spectrometry (AP-MS) and *in vitro* by SPR and AUC, the latter pointing to a stoichiometric complex. Furthermore, when both proteins are co-purified, RhpA is able to assist *Hp*RNase R in dsRNA substrate degradation *in vitro*. These results demonstrate that *Hp*RNase R and RhpA indeed form a functional complex. We hypothesize that this complex might be widespread within the phylum *Campylobacterota*, as most of these bacteria harbor both an RNase R ortholog with similar domain characteristics

as *Hp*RNase R and a single protein from the family of the DEAD-box RNA helicases.

In *Pseudomonas syringae*, a psychrophilic organism, the RNA degradosome was shown to comprise RNase E, a DEAD box helicase and RNase R, whose sequence is comparable to that of *Ec*RNase R. In that case, it was proposed that RNase R replaces the classical PNPase of the RNase E-based degradosomes (40). In *H. pylori*, we previously showed that RNase J forms a functional RNA degradosome with the RhpA helicase (2). This raises the question as to whether *Hp*RNase R might be an additional minor partner of this degradosome or whether RhpA can be engaged into two alternative complexes. More work is needed to answer to this question. However, we found, that independently of RhpA, *Hp*RNase R localizes to the inner membrane of *H. pylori* just like the two RNA degradosome partners, RhpA and RNase J (11). Interestingly, one of the putative RNase R interactors identified by AP-MS is the membrane scaffolding protein flotillin FloA (HPB8_1315) which we previously found to promote the compartmentalization of the RNA degradosome of *H. pylori* (11). Altogether, these data are in favor of an 'RNA degradation hub' that would be compartmentalized at the membrane of *H. pylori*.

Several approaches have been pursued to assess the role of *Hp*RNase R in *H. pylori*. First, we observed no change in the amounts of the *Hp*RNase R protein as a function of growth phase, during growth at 33°C (the lowest temperature that supports *H. pylori* growth) or after cold shock at 4°C. This contrasts with *Ec*RNase R which is regulated at

both transcriptional and stability level by growth phase and cold shock. In *E. coli*, the regulation is partly due to the interaction of *Ec*RNase R with the *trans*-translation machinery, *tm*RNA-SmpB ([72]), which in turn favors the interaction with and degradation by the Lon and HslUV proteases ([73]). In *H. pylori*, the absence of such *Hp*RNase R regulation might be related to the lack of the domains that mediate this regulation [the K/R-rich and S1 C-terminal domains ([72])]. In agreement with this, SmpB, HslU and Lon were not detected as *Hp*RNase R interactors by AP-MS. Helicase activities are generally crucial for growth at lower temperatures, where RNA secondary structures are stabilized; since *Hp*RNase R is not efficient in degrading dsRNA structures and needs to associate with a helicase, it makes sense that it does not need to be regulated by cold shock. Nevertheless, as we previously showed, the RhpA helicase plays a major role at 33°C since it is essential for growth of *H. pylori* at this temperature.

RNA-Seq was performed to identify the targets of *Hp*RNase R. We found only 11 differentially expressed genes in a Δ*rnr* mutant. Although we cannot exclude that *Hp*RNase R is more active under conditions different from those tested here, we conclude that this enzyme does not play a major role in the control of RNA decay. It seems, as we previously showed, that RNase J, another *H. pylori* ribonuclease, is the major actor in RNA degradation ([7]). Surprisingly, we found no overlap between our targets and those of the previous publication reporting the changes in *H. pylori* Δ*rnr* transcriptome ([41]), which might be attributed to the use of another strain.

Based on our data, we propose that *Hp*RNase R has evolved an interaction with RhpA in order to carry out some of its functions on partially structured RNAs. In agreement with this, all the *Hp*RNase R targets, including the LpxC LPS biosynthesis gene, are similarly dysregulated in the Δ*rnr* and Δ*rhpA* strains. It is interesting to note that, in *E. coli*, LPS-biosynthesis genes were found to be regulated by RNase II, the other 3′-5′ exoribonuclease of the same family as RNase R that does not exist in *H. pylori* ([74]). RhpA has many other targets, mostly mRNAs but also asRNAs and sRNAs.

In *Streptococcus pyogenes*, few RNase R targets have been identified, and several of those are also contained within the PNPase regulon, but whether its RNase R retains the helicase activity has not been addressed ([75,76]). In contrast, 202 genes are differentially regulated in the *E. coli* Δ*rnr* mutant ([42]).

We also asked whether *Hp*RNase R might be required for the maturation of stable RNAs such as *tm*RNA or rRNAs, which would not be detected by RNA-Seq. *Ec*RNase R plays a central role in *tm*RNA function ([77]). In *H. pylori*, we found no changes in the *tm*RNA 3′-extremity. Since we previously established that *trans*-translation is indispensable for *H. pylori* viability ([71]) and because RNase R is not essential, we conclude that other RNase(s) are responsible for the degradation of defective mRNAs following *trans*-translation in *H. pylori*. We also found that several ribosomal proteins interact with *Hp*RNase R (Supplementary Table S4). Whereas, in *E. coli,* ribosomes were shown to stabilize RNase R protein ([38]), we do not know whether this

is also the case in *H. pylori*. However, using 3′-RACE we found a minor role of *Hp*RNase R in the maturation of the 5S rRNA, while we clearly detected the defect in 16S rRNA maturation that was previously reported in a Δ*rhpA* mutant ([10]). Even so, our results do not exclude the possibility that RNase R might act by trimming the 3′-end of different RNA species in the cell, as seems to be the case in *S. pyogenes* ([76]), which could have effects at the proteomic level and for RNA maturation.

In conclusion, we have described a novel type of RNase R, *Hp*RNase R, that lacks the helicase domains and activity and thus the ability to degrade dsRNA substrates. In order to compensate for this defect, we propose that *Hp*RNase R has evolved to co-opt RhpA, the DEAD-box RNA helicase of *H. pylori*, to assist some of its functions.

DATA AVAILABILITY

RNA-Seq data can be found in Annotare under the accession number E-MTAB-10045. The mass spectrometry proteomics data have been deposited to the ProteomeXchange Consortium via the PRIDE ([78]) partner repository with the dataset identifier PXD023837.

SUPPLEMENTARY DATA

Supplementary Data are available at NAR Online.

ACKNOWLEDGEMENTS

FUNDING

REFERENCES

1. Tejada-Arranz,A., de Crécy-Lagard,V. and de Reuse,H. (2020) Bacterial RNA degradosomes: molecular machines under tight control. *Trends Biochem. Sci.*, **45**, 42–57.
2. Redko,Y., Aubert,S., Stachowicz,A., Lenormand,P., Namane,A., Darfeuille,F., Thibonnier,M. and De Reuse,H. (2013) A minimal bacterial RNase J-based degradosome is associated with translating ribosomes. *Nucleic. Acids. Res.*, **41**, 288–301.
3. Waite,D.W., Vanwonterghem,I., Rinke,C., Parks,D.H., Zhang,Y., Takai,K., Sievert,S.M., Simon,J., Campbell,B.J., Hanson,T.E. *et al.* (2017) Comparative genomic analysis of the class Epsilonproteobacteria and proposed reclassification to Epsilonbacteraeota (phyl. nov.). *Front. Microbiol.*, **8**, 682.
4. Waite,D.W., Vanwonterghem,I., Rinke,C., Parks,D.H., Zhang,Y., Takai,K., Sievert,S.M., Simon,J., Campbell,B.J., Hanson,T.E. *et al.* (2018) Addendum: Comparative genomic analysis of the class Epsilonproteobacteria and proposed reclassification to Epsilonbacteraeota (phyl. nov.). *Front. Microbiol.*, **9**, 772.
5. Amieva,M. and Peek,R.M. (2016) Pathobiology of *Helicobacter pylori*–induced gastric cancer. *Gastroenterology*, **150**, 64–78.
6. De la Cruz,M.A., Ares,M.A., von Bargen,K., Panunzi,L.G., Martínez-Cruz,J., Valdez-Salazar,H.A., Jiménez-Galicia,C. and Torres,J. (2017) Gene expression profiling of transcription factors of *Helicobacter pylori* under different environmental conditions. *Front. Microbiol.*, **8**, 615.
7. Redko,Y., Galtier,E., Arnion,H., Darfeuille,F., Sismeiro,O., Coppée,J.-Y., Médigue,C., Weiman,M., Cruveiller,S. and De Reuse,H. (2016) RNase J depletion leads to massive changes in mRNA abundance in *Helicobacter pylori*. *RNA Biol.*, **13**, 243–253.
8. Sharma,C.M., Hoffmann,S., Darfeuille,F., Reignier,J., Findeiß,S., Sittka,A., Chabas,S., Reiche,K., Hackermüller,J., Reinhardt,R. *et al.* (2010) The primary transcriptome of the major human pathogen Helicobacter pylori. *Nature*, **464**, 250–255.
9. Pernitzsch,S.R. and Sharma,C.M. (2012) Transcriptome complexity and riboregulation in the human pathogen *Helicobacter pylori*. *Front. Cell. Infect. Microbiol.*, **2**, 14.
10. El Mortaji,L., Aubert,S., Galtier,E., Schmitt,C., Anger,K., Redko,Y., Quentin,Y. and De Reuse,H. (2018) The sole DEAD-box RNA helicase of the gastric pathogen Helicobacter pylori is essential for colonization. *MBio*, **9**, e02071-17.
11. Tejada-Arranz,A., Galtier,E., El Mortaji,L., Turlin,E., Ershov,D. and De Reuse,H. (2020) The RNase J-Based RNA degradosome is compartmentalized in the gastric pathogen *Helicobacter pylori*. *MBio*, **11**, e01173-20.
12. Cheng,Z.-F. and Deutscher,M.P. (2005) An important role for RNase R in mRNA decay. *Mol. Cell*, **17**, 313–318.
13. Cheng,Z.-F. and Deutscher,M.P. (2003) Quality control of ribosomal RNA mediated by polynucleotide phosphorylase and RNase R. *Proc. Natl. Acad. Sci. U.S.A.*, **100**, 6388–6393.
14. Sulthana,S. and Deutscher,M.P. (2013) Multiple exoribonucleases catalyze maturation of the 3′ terminus of 16S ribosomal RNA (rRNA). *J. Biol. Chem.*, **288**, 12574–12579.
15. Dos Santos,R.F., Andrade,J.M., Pissarra,J., Deutscher,M.P. and Arraiano,C.M. (2020) Hfq and RNase R mediate rRNA processing and degradation in a novel RNA quality control process. *MBio*, **11**, e02398-20.
16. Cairrão,F., Cruz,A., Mori,H. and Arraiano,C.M. (2003) Cold shock induction of RNase R and its role in the maturation of the quality control mediator SsrA/tmRNA. *Mol. Microbiol.*, **50**, 1349–1360.
17. Domingues,S., Moreira,R.N., Andrade,J.M., Dos Santos,R.F., Bárria,C., Viegas,S.C. and Arraiano,C.M. (2015) The role of RNase R in trans-translation and ribosomal quality control. *Biochimie*, **114**, 114–118.
18. Zhang,Y., Burkhardt,D.H., Rouskin,S., Li,G.-W., Weissman,J.S. and Gross,C.A. (2018) A stress response that monitors and regulates mRNA structure is central to cold shock adaptation. *Mol. Cell*, **70**, 274–286.
19. Mohanty,B.K. and Kushner,S.R. (2018) Enzymes involved in posttranscriptional RNA metabolism in Gram-negative bacteria. In: *Regulating with RNA in Bacteria and Archaea*. American Society of Microbiology, Vol. **6**, pp. 19–35.
20. Matos,R.G., Casinhas,J., Bárria,C., dos Santos,R.F., Silva,I.J. and Arraiano,C.M. (2017) The role of ribonucleases and sRNAs in the virulence of foodborne pathogens. *Front. Microbiol.*, **8**, 910.
21. Bárria,C., Domingues,S. and Arraiano,C.M. (2019) Pneumococcal RNase R globally impacts protein synthesis by regulating the amount of actively translating ribosomes. *RNA Biol.*, **16**, 211–219.
22. Mohanty,B.K. and Kushner,S.R. (2003) Genomic analysis in Escherichia coli demonstrates differential roles for polynucleotide phosphorylase and RNase II in mRNA abundance and decay. *Mol. Microbiol.*, **50**, 645–658.
23. Mohanty,B. and Kushner,S. (2010) Processing of the *Escherichia coli* leuX tRNA transcript, encoding tRNA(Leu5), requires either the 3′-5′ exoribonuclease polynucleotide phosphorylase or RNase P to remove the Rho-independent transcription terminator. *Nucleic. Acids. Res.*, **38**, 597–607.
24. Basturea,G.N., Zundel,M.A. and Deutscher,M.P. (2011) Degradation of ribosomal RNA during starvation: comparison to quality control during steady-state growth and a role for RNase PH. *RNA*, **17**, 338–345.
25. Awano,N., Rajagopal,V., Arbing,M., Patel,S., Hunt,J., Inouye,M. and Phadtare,S. (2010) *Escherichia coli* RNase R has dual activities, helicase and RNase. *J. Bacteriol.*, **192**, 1344–152.
26. Haddad,N., Matos,R.G., Pinto,T., Rannou,P., Cappelier,J.-M., Prévost,H. and Arraiano,C.M. (2014) The RNase R from *Campylobacter jejuni* has unique features and is involved in the first steps of infection. *J. Biol. Chem.*, **289**, 27814–27824.
27. Cheng,Z.-F. and Deutscher,M.P. (2002) Purification and characterization of the *Escherichia coli* exoribonuclease RNase R. *J. Biol. Chem.*, **277**, 21624–21629.
28. Hossain,S.T. and Deutscher,M.P. (2016) Helicase activity plays a crucial role for RNase R function in vivo and for RNA metabolism. *J. Biol. Chem.*, **291**, 9438–9443.
29. Hossain,S.T., Malhotra,A. and Deutscher,M.P. (2015) The helicase activity of ribonuclease R is essential for efficient nuclease activity. *J. Biol. Chem.*, **290**, 15697–15706.
30. Hossain,S.T., Malhotra,A. and Deutscher,M.P. (2016) How RNase R degrades structured RNA. *J. Biol. Chem.*, **291**, 7877–7887.
31. Vincent,H.A. and Deutscher,M.P. (2009) The roles of individual domains of RNase R in substrate binding and exoribonuclease activity. The nuclease domain is sufficient for digestion of structured RNA. *J. Biol. Chem.*, **284**, 486–494.
32. Chu,L.-Y., Hsieh,T.-J., Golzarroshan,B., Chen,Y.-P., Agrawal,S. and Yuan,H.S. (2017) Structural insights into RNA unwinding and degradation by RNase R. *Nucleic Acids Res.*, **45**, 12015–12024.
33. Matos,R.G., Barbas,A., Gómez-Puertas,P. and Arraiano,C.M. (2011) Swapping the domains of exoribonucleases RNase II and RNase R: conferring upon RNase II the ability to degrade ds RNA. *Proteins*, **79**, 1853–167.
34. Andrade,J.M., Cairrão,F. and Arraiano,C.M. (2006) RNase R affects gene expression in stationary phase: regulation of ompA. *Mol. Microbiol.*, **60**, 219–228.
35. Barria,C., Malecki,M. and Arraiano,C.M. (2013) Bacterial adaptation to cold. *Microbiology*, **159**, 2437–2443.
36. Chen,C. and Deutscher,M.P. (2005) Elevation of RNase R in response to multiple stress conditions. *J. Biol. Chem.*, **280**, 34393–34396.
37. Malecki,M., Bárria,C. and Arraiano,C.M. (2014) Characterization of the RNase R association with ribosomes. *BMC Microbiol.*, **14**, 34.
38. Liang,W. and Deutscher,M.P. (2013) Ribosomes regulate the stability and action of the exoribonuclease RNase R. *J. Biol. Chem.*, **288**, 34791–34798.
39. Carabetta,V.J., Silhavy,T.J. and Cristea,I.M. (2010) The response regulator SprE (RssB) is required for maintaining poly(A) polymerase I-degradosome association during stationary phase. *J. Bacteriol.*, **192**, 3713–3721.
40. Purusharth,R.I., Klein,F., Sulthana,S., Jäger,S., Jagannadham,M.V., Evguenieva-Hackenberg,E., Ray,M.K. and Klug,G. (2005) Exoribonuclease R interacts with endoribonuclease E and an RNA helicase in the psychrotrophic bacterium *Pseudomonas syringae* Lz4W. *J. Biol. Chem.*, **280**, 14572–14578.
41. Tsao,M.-Y., Lin,T.-L., Hsieh,P.-F. and Wang,J.-T. (2009) The 3′-to-5′ exoribonuclease (encoded by HP1248) of *Helicobacter pylori* regulates motility and apoptosis-inducing genes. *J. Bacteriol.*, **191**, 2691–2702.

42. Pobre,V. and Arraiano,C.M. (2015) Next generation sequencing analysis reveals that the ribonucleases RNase II, RNase R and PNPase affect bacterial motility and biofilm formation in E. coli. *BMC Genomics*, **16**, 72.

43. Farnbacher,M., Jahns,T., Willrodt,D., Daniel,R., Haas,R., Goesmann,A., Kurtz,S. and Rieder,G. (2010) Sequencing, annotation, and comparative genome analysis of the gerbil-adapted Helicobacter pylori strain B8. *BMC Genomics*, **11**, 335.

44. McClain,M.S., Shaffer,C.L., Israel,D.A., Peek,R.M. and Cover,T.L. (2009) Genome sequence analysis of *Helicobacter pylori* strains associated with gastric ulceration and gastric cancer. *BMC Genomics*, **10**, 3.

45. Sambrook,J., Russell,D.W. and David,W. (2001) In: *Molecular Cloning: A Laboratory Manual*, Cold Spring Harbor Laboratory Press.

46. Gibson,D.G., Young,L., Chuang,R.-Y., Venter,J.C., Hutchison,C.A. and Smith,H.O. (2009) Enzymatic assembly of DNA molecules up to several hundred kilobases. *Nat. Methods*, **6**, 343–345.

47. Bury-Mone,S., Skouloubris,S., Dauga,C., Thiberge,J.-M., Dailidiene,D., Berg,D.E., Labigne,A. and De Reuse,H. (2003) Presence of active aliphatic amidases in *Helicobacter* species able to colonize the stomach. *Infect. Immun.*, **71**, 5613–5622.

48. Notredame,C., Higgins,D.G. and Heringa,J. (2000) T-Coffee: a novel method for fast and accurate multiple sequence alignment. *J. Mol. Biol.*, **302**, 205–217.

49. Waterhouse,A.M., Procter,J.B., Martin,D.M.A., Clamp,M. and Barton,G.J. (2009) Jalview Version 2 – a multiple sequence alignment editor and analysis workbench. *Bioinformatics*, **25**, 1189–1191.

50. Parks,D.H., Chuvochina,M., Chaumeil,P.-A., Rinke,C., Mussig,A.J. and Hugenholtz,P. (2020) A complete domain-to-species taxonomy for Bacteria and Archaea. *Nat. Biotechnol.*, **38**, 1079–1086.

51. Seemann,T. (2014) Prokka: rapid prokaryotic genome annotation. *Bioinformatics*, **30**, 2068–2069.

52. Eddy,S.R. (2011) Accelerated profile HMM searches. *PLoS Comput. Biol.*, **7**, e1002195.

53. Price,M.N., Dehal,P.S. and Arkin,A.P. (2009) FastTree: computing large minimum evolution trees with profiles instead of a distance matrix. *Mol. Biol. Evol.*, **26**, 1641–1650.

54. Letunic,I. and Bork,P. (2019) Interactive Tree Of Life (iTOL) v4: recent updates and new developments. *Nucleic Acids Res.*, **47**, W256–W259.

55. Katoh,K. and Standley,D.M. (2013) MAFFT multiple sequence alignment software version 7: improvements in performance and usability. *Mol. Biol. Evol.*, **30**, 772–80.

56. Capella-Gutierrez,S., Silla-Martinez,J.M. and Gabaldon,T. (2009) trimAl: a tool for automated alignment trimming in large-scale phylogenetic analyses. *Bioinformatics*, **25**, 1972–1973.

57. Matos,R.G., Barbas,A. and Arraiano,C.M. (2009) RNase R mutants elucidate the catalysis of structured RNA: RNA-binding domains select the RNAs targeted for degradation. *Biochem. J.*, **423**, 291–301.

58. Karimova,G., Pidoux,J., Ullmann,A. and Ladant,D. (1998) A bacterial two-hybrid system based on a reconstituted signal transduction pathway. *Proc. Natl. Acad. Sci. U.S.A.*, **95**, 5752–5756.

59. Miller,J.H. (1972) In: *Experiments in Molecular Genetics*, Cold Spring Harbor Laboratory.

60. Schuck,P. (2000) Size-distribution analysis of macromolecules by sedimentation velocity ultracentrifugation and Lamm equation modeling. *Biophys. J.*, **78**, 1606–1619.

61. Laue,T., Shah,B., Ridgeway,T. and Pelletier,S. (1992) Computer-aided interpretation of analytical sedimentation data for proteins. In: Harding,S.E., Rowe,A. and Horton,J. (eds). *Analytical Ultracentrifugation in Biochemistry and Polymer Science*. Royal Society of Chemistry, Cambridge, pp. 90–125.

62. Skouloubris,S., Labigne,A. and De Reuse,H. (2001) The AmiE aliphatic amidase and AmiF formamidase of Helicobacter pylori: natural evolution of two enzyme paralogues. *Mol. Microbiol.*, **40**, 596–609.

63. Cokelaer,T., Desvillechabrol,D., Legendre,R. and Cardon,M. (2017) 'Sequana': a set of Snakemake NGS pipelines. *J. Open Source Softw.*, **2**, 352.

64. Köster,J. and Rahmann,S. (2012) Snakemake–a scalable bioinformatics workflow engine. *Bioinformatics*, **28**, 2520–2522.

65. Martin,M. (2011) Cutadapt removes adapter sequences from high-throughput sequencing reads. *EMBnet.journal*, **17**, 10.

66. Langmead,B. and Salzberg,S.L. (2012) Fast gapped-read alignment with Bowtie 2. *Nat. Methods*, **9**, 357–359.

67. Liao,Y., Smyth,G.K. and Shi,W. (2014) featureCounts: an efficient general purpose program for assigning sequence reads to genomic features. *Bioinformatics*, **30**, 923–930.

68. Ewels,P., Magnusson,M., Lundin,S. and Käller,M. (2016) MultiQC: summarize analysis results for multiple tools and samples in a single report. *Bioinformatics*, **32**, 3047–3048.

69. Love,M.I., Huber,W. and Anders,S. (2014) Moderated estimation of fold change and dispersion for RNA-seq data with DESeq2. *Genome Biol.*, **15**, 550.

70. Varet,H., Brillet-Guéguen,L., Coppée,J.-Y. and Dillies,M.-A. (2016) SARTools: a DESeq2- and EdgeR-based R pipeline for comprehensive differential analysis of RNA-Seq data. *PLoS One*, **11**, e0157022.

71. Thibonnier,M., Thiberge,J.-M., De Reuse,H., Myers,G. and Nedrud,J. (2008) Trans-translation in *Helicobacter pylori*: essentiality of ribosome rescue and requirement of protein tagging for stress resistance and competence. *PLoS One*, **3**, e3810.

72. Liang,W. and Deutscher,M.P. (2010) A novel mechanism for ribonuclease regulation: transfer-messenger RNA (tmRNA) and its associated protein SmpB regulate the stability of RNase R. *J. Biol. Chem.*, **285**, 29054–29058.

73. Liang,W. and Deutscher,M.P. (2012) Transfer-messenger RNA-SmpB protein regulates ribonuclease R turnover by promoting binding of HslUV and Lon proteases. *J. Biol. Chem.*, **287**, 33472–33479.

74. Pobre,V., Barahona,S., Dobrzanski,T., Steffens,M.B.R. and Arraiano,C.M. (2019) Defining the impact of exoribonucleases in the shift between exponential and stationary phases. *Sci. Rep.*, **9**, 16271.

75. Lécrivain,A.-L., Le Rhun,A., Renault,T.T., Ahmed-Begrich,R., Hahnke,K. and Charpentier,E. (2018) In vivo 3′-to-5′ exoribonuclease targetomes of *Streptococcus pyogenes*. *Proc. Natl. Acad. Sci. U.S.A.*, **115**, 11814–11819.

76. Broglia,L., Lécrivain,A.-L., Renault,T.T., Hahnke,K., Ahmed-Begrich,R., Le Rhun,A. and Charpentier,E. (2020) An RNA-seq based comparative approach reveals the transcriptome-wide interplay between 3′-to-5′ exoRNases and RNase Y. *Nat. Commun.*, **11**, 1587.

77. Richards,J., Mehta,P. and Karzai,A.W. (2006) RNase R degrades non-stop mRNAs selectively in an SmpB-tmRNA-dependent manner. *Mol. Microbiol.*, **62**, 1700–1712.

78. Perez-Riverol,Y., Csordas,A., Bai,J., Bernal-Llinares,M., Hewapathirana,S., Kundu,D.J., Inuganti,A., Griss,J., Mayer,G., Eisenacher,M. *et al.* (2019) The PRIDE database and related tools and resources in 2019: improving support for quantification data. *Nucleic Acids Res.*, **47**, D442–D450.

79. Frazão,C., McVey,C.E., Amblar,M., Barbas,A., Vonrhein,C., Arraiano,C.M. and Carrondo,M.A. (2006) Unravelling the dynamics of RNA degradation by ribonuclease II and its RNA-bound complex. *Nature*, **443**, 110–114.